Scientific Research Communications

Research Article

Sci. Res. Comm. (2022)
Volume 2, Issue 2
doi: 10.52460/src.2022.008

Application of the WASP Model for Assessment of Aeration Impact on Water Quality of Porsuk River, Turkey

Emre Dumlu[1,*] **Şebnem Elçi**[1]

[1] Civil Engineering Department, İzmir Institute of Technology, 35430 Urla/İzmir
[*] Corresponding author: emredumlu@iyte.edu.tr

Received: 15.08.2022 Accepted: 20.10.2022

Abstract

Porsuk Stream is the longest branch of the Sakarya Basin which originates from Murat Mountain and bypasses the provinces of Kutahya and Eskisehir. Based on recent increasing pollution concentrations reported in the literature, the main river is experiencing problems with decreased water quality. In this study, hydrodynamics and water quality parameters are simulated in the Porsuk River via the application of the Water Quality Analysis Simulation Program (WASP) using the available flow and meteorological data. After the validation of the hydrodynamics along the main river, water quality parameters are simulated using the eutrophication module. Simulation of dissolved oxygen concentrations pointed out hypoxia, especially at two locations; Kutahya-Reservoir1 and Alpu-Guroluk segments where dissolved oxygen values stayed well below the standard limits throughout the year. As a mitigation option, aeration applications at these two stations are proposed and the effects of aeration on the simulated parameters of dissolved oxygen, phosphorus and nitrate concentrations are investigated. Aeration at two segments has significantly improved the dissolved oxygen concentrations (from ~3 mg/l to >14 mg/l) whereas it has a more subtle effect on nitrate and phosphorus concentrations.

Keywords: WASP model, Porsuk River, water quality, aeration

1. Introduction

High nutrient concentrations and high turbidity often result in cyanobacterial blooms in water systems. Cyanobacterial blooms are likely to increase in frequency and intensity in response to climate change and eutrophication factors. The presence of cyanobacteria above 2000 cells/ml in potable water supplies can cause taste and odor problems, which increase the cost of water treatment. Higher levels of cyanobacteria (>50 000 cells/ml) render surface waters unsuitable for contact whereas very high levels, as occur in floating blooms, can result in fish kills and are potentially lethal when consumed (Hickey and Gibbs, 2009). Increases in toxins are all impacts of planktonic cyanobacterial blooms, whereas the bloom collapses may result in the creation of ammonia (Havens, 2008). It has been challenging to come up with complete explanations for why these species have thrived (Hyenstrand et al., 1998). A relationship has been found that cyanobacterial dominance (>50% of the phytoplankton population) increases rapidly when total P increases (Downing et al., 2001).

Freshwater systems are vital in supplying water for drinking, growing crops, manufacturing and energy and transport. Therefore, seasonal changes of water quality largely affect not only

the watershed area, but also ecosystem in region of interest. In recent years, excessive population growth, rapid increase in urbanization and industrialization, accompanied by the adverse effects of climate change, put increased pressure on the natural water resources and resulted in pollution of the existing resources that are already limited.

Water quality models are essential tools for effective management of water resources and play an important role in decision-making by providing water quality simulations and by allowing testing of a variety of management actions. Over the years, they have become an important tool for identifying water pollution and the final fate and behaviors of pollutants in a water environment (Wang et al., 2009). A wide range of models from simple to highly sophisticated numerical applications for simulating water quality has been developed. Burigato Costa et al. (2019) provided a review of the water quality models and stated that based on their review of the water quality-related studies conducted in the past 21 years water quality simulations: An aquatic ecosystem and toxicant simulation model (AQUATOX), two-dimensional hydrodynamic and water-quality model (CE-QUAL-W2), enviromental fluid dynamics code (EFDC), one-dimensional steady-state water quality models (QUALs), soil and water assessment tool (SWAT), spatially referenced regressions on watershed (SPARROW), and the water quality analysis simulation program (WASP) have been widely applied around the world. WASP, supported and developed by the US Environmental Protection Agency (USEPA), is a multi-dimensional and dynamic water quality modeling program. The model can be used to analyze a variety of water quality problems in ponds, streams, lakes, reservoirs, rivers, estuaries, and coastal waters. The time-varying processes of advection, dispersion, point and diffuse mass loading and boundary exchange are represented in the model.

The numerical model selected in this study, the water quality analysis simulation program (WASP); is a differential, spatially resolved, mass balance, fate and transport modeling framework structured to allow users to simulate concentrations of environmental contaminants in surface waters and bottom sediments (Ambrose et al., 1993). Water quality analyses are implemented for the water year of 2015 (10/1/2014 - 9/30/2015) using the WASP model. The Porsuk main river is divided into 25 segments in total, based on the available monitored water quality data. In Kose et. al, (2016), water quality parameters were collected from 18 stations located on the Porsuk Stream in 2015 and some important physicochemical parameters were investigated to determine the water quality of the stream. While dividing the main river into segments, segment length is set to 20 km at most, and the segments are named considering the starting and the ending locations. The average width and length of each segment are then calculated. For calibration of the model, all the available stations; Beskaris, Porsuk Ciftligi, Calca, Esenkara, Parsibey and Kiranharmani are considered, and the flow rates are obtained from The General Directorate of State Hydraulic Works (DSI) and The General Directorate of Electrical Power Resources Survey and Development Administration (EIE). Once the numerical model is calibrated based on flow rates, water quality parameters are simulated. Observed dissolved oxygen, phosphorus and nitrate concentrations are also implemented to validate the model. In the final part, aeration is proposed as mitigation for hypoxia observed at some stations and the effects of aeration on the simulated results are discussed.

2. Methodology

2.1. Study Site

Porsuk Stream Basin, a branch of the Sakarya river extends 201 km in the East-West direction in Northwest Anatolia and reaches 135 km of distance in the south direction and covers a precipitation area of 10,869 km² (Tekkanat and Sarış, 2015). It originates from Murat Mountain and flows into the Sakarya River after passing through Kutahya and Eskisehir provinces. The

study area, segmentation of the river and available stations along the river are given in Figure 1 (Dumlu and Elçi, 2022). In Figure 1, stations where water quality parameters were monitored by Köse et al. (2016), are presented with blue dots, stations where flow data are monitored by DSI are marked with brown dots. Additional stations added for the segmentation are shown by green dots. The reference coordinate system is arranged to WGS 84/Pseudo-Mercator (EPSG:3857).

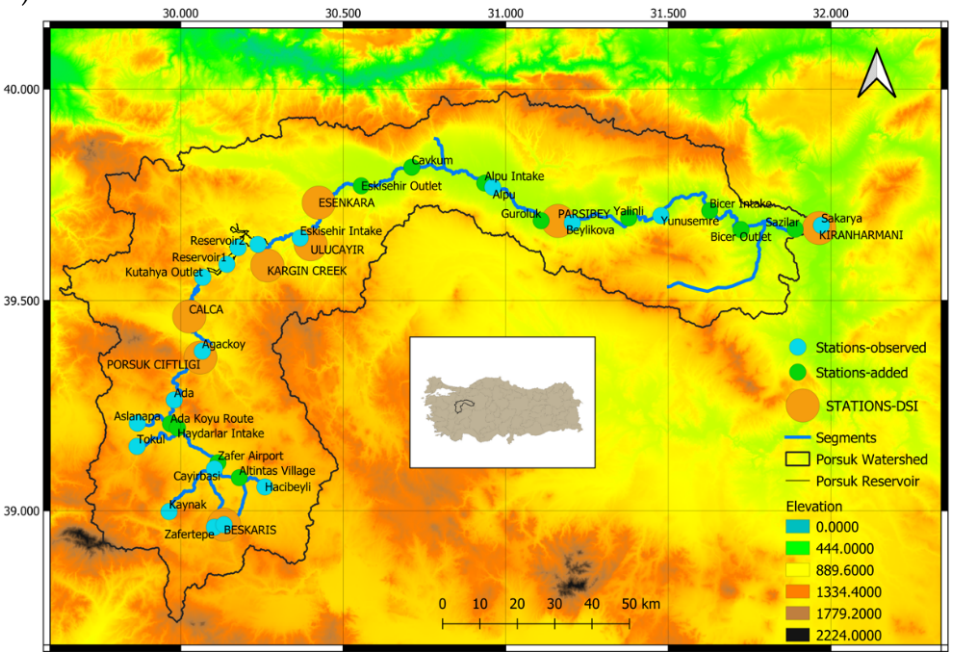

Figure 1: Porsuk watershed and locations of stations considered in the model

2.2 Data Sources

The meteorological data are downloaded from Giovanni for the nearest stations: Alpu and Zafer Airport. 'Giovanni', an open data portal of NASA between 10/1/2014-09/30/2015 (https://giovanni.gsfc.nasa.gov/giovanni, accessed on 25th July 2022). The Goddard Earth Sciences Data and Information Services Center (GES DISC) has created web-based GES DISC Interactive Online Visualization and Analysis Infrastructure, (Giovanni), to enable analysis of satellite remotely sensed meteorological, oceanographic, and hydrologic data sets. The AIRS3STD model is used for the air temperature in the availability of data bounding box 30.5E, 39.59N, while the GLDAS model was used for the available data bounding box 29.875N, 39.625E for both wind speed and solar radiation time series, respectively.

The flow rate data at Beskaris, Porsuk Ciftligi, Calca, Esenkara, Parsibey, and Kiranharmani stations are obtained from the State Hydraulic Works for the water year of 2015.

The observed air temperature, wind speed and solar radiation data for the water year of 2015 are presented in Figures 2,3 and 4.

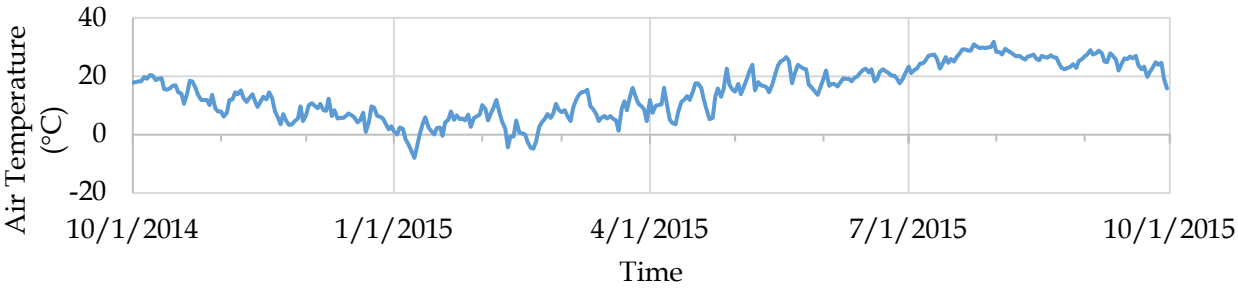

Figure 2: Monitored air temperatures

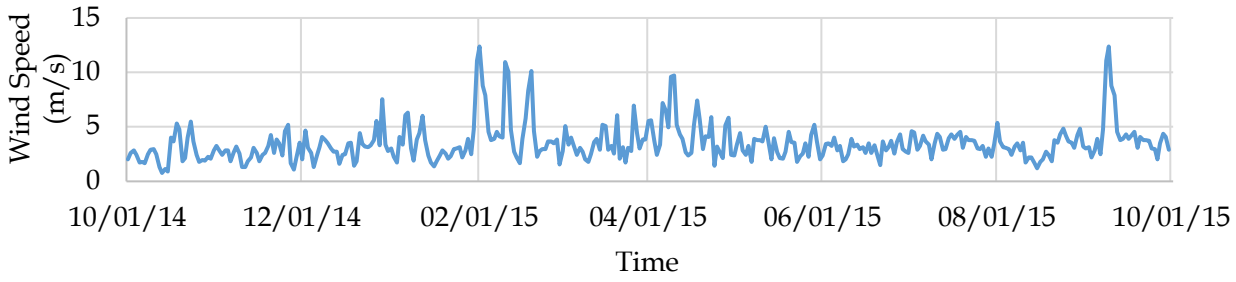

Figure 3: Monitored wind speed data

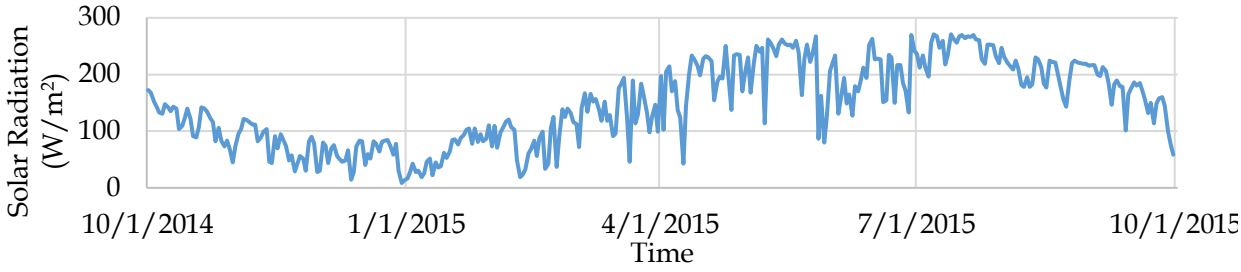

Figure 4: Monitored solar radiation data

The validity of the data (Giovanni) is tested by comparing the data monitored at the two meteorological stations close to the study site. Daily air temperatures from ALPU and Zafer Airport stations are obtained and averaged and then compared with the data downloaded from Giovanni for our study region (Figure 5). Results indicated that the data from Giovanni overpredicted the monitored data but the correlation between two data sets was high having R^2 of 0.90.

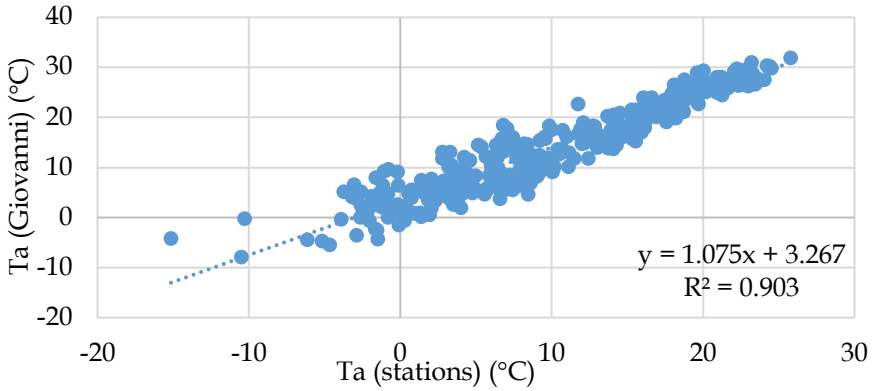

Figure 5. Comparison of monitored air temperatures with the data downloaded from Giovanni

Next, we obtained the monitored water temperature data for Besdegirmen station located in the study site from the State Hydraulic Works. Water temperature data was available for seven years (2006-2013) and collected once a month. For the specific dates when the monitoring took place, daily water temperatures are derived from the monitored daily air temperatures for the stations. Water temperatures monitored once a month at the suspended sediment monitoring station of Besdegirmen are obtained between 2006-2012 and are used to issue a relation between the measured water temperatures and the air temperatures for the corresponding

dates of the measurements. The equation relating air temperatures to water temperatures is derived as in Eq (1):

$$T_w = 0.487 * T_a + 8.6027 \quad (1)$$

where T_w is the water temperature (°C) while, T_a is the air temperature (°C).

Next, we compared water temperatures predicted by the air temperature data from the monitoring stations and Giovanni with the monitored water temperatures (Figure 6). Results showed that the later comparison had a better correlation with the monitored water temperature data. This analysis showed that meteorological data downloaded from Giovanni can be used for predicting water temperature in the streams and are well correlated with the monitored meteorological data at the study site (Figure 7).

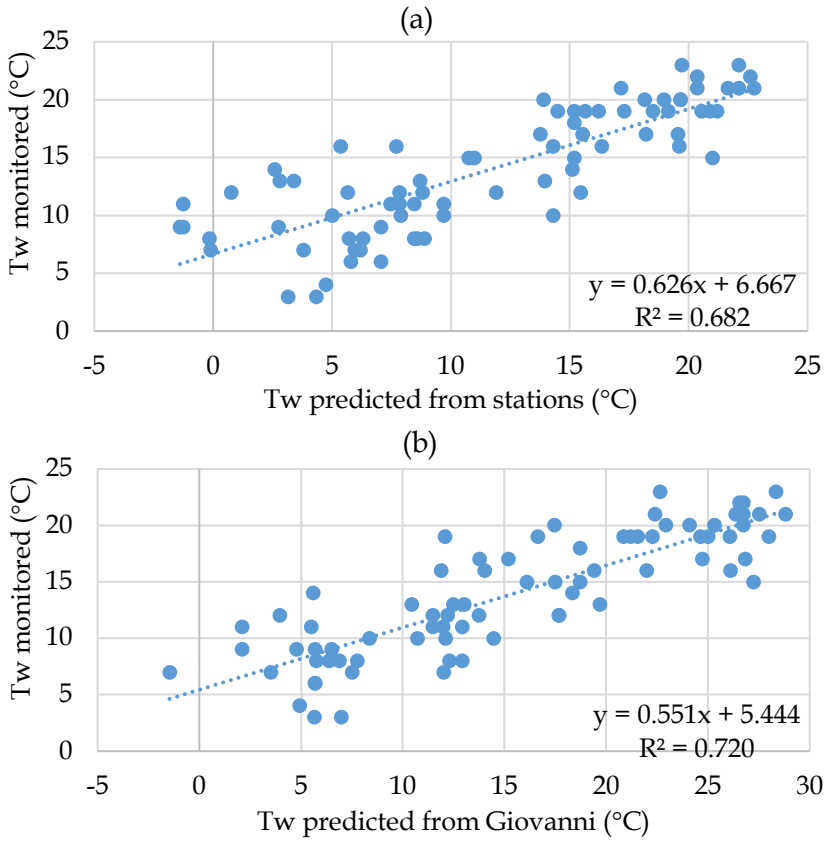

Figure 6. (a) Comparison of predicted water temperatures by the air temperature data from the monitoring stations with the monitored water temperatures, (b) Comparison of predicted water temperatures by the data from Giovanni with the monitored water temperatures

Eq. (1) is then used to find the values of daily water temperature data to be used as input to the model for the water year of 2015. The data presented in Figure 8 are used as water temperature time series input to the model for the simulation period.

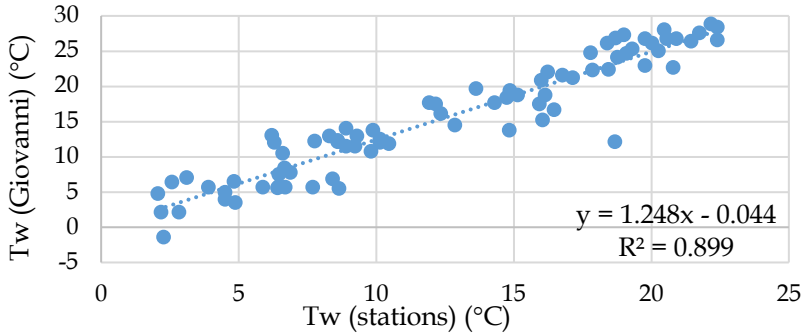

Figure 7. Comparison of water temperatures predicted using the air temperature data from the monitoring stations with the water temperatures predicted using the air temperature data from Giovanni

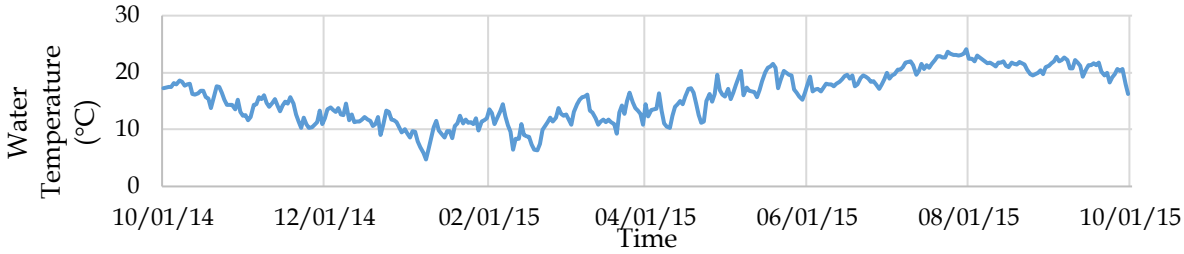

Figure 8. Water Temperature Time Series used in the simulations

2.3. Application of the WASP Model

WASP also can be linked with hydrodynamic and sediment transport models that can provide flows, depths, velocities, temperature, salinity and sediment fluxes. WASP contains four layers representing different parts of water ecosystems. These layers are defined as 1) The water column in contact with the atmosphere, 2) The water column non-contact with the atmosphere, 3) The underlying benthos in contact with water, 4) The sediment bed non-contact with water. When the conservation of mass and momentum are solved for both water and solids between the layers, flow and transport in the water column, transport in the porous media of the bed sediment, transport in the water column via settling/re-suspension and transport with rainfall/evaporation are considered. Although the model cannot execute hydrologic computations, it can be linked to hydrologic models such as HSPF and SWIMM and can be linked to hydrodynamic models through input files. When WASP is used alone, it solves the hydrodynamics using the kinematic wave equation. It can also transfer data to the central database system developed by the EPA (Ambrose et al., 1993).

Water quality processes are represented in special kinetic subroutines that are either chosen from a library or written by the user. WASP is structured to permit easy substitution of kinetic subroutines into the overall package to form problem-specific models. WASP8 comes with four modules: TOXI for simulation of toxicants and EUTRO for simulation of conventional water quality, including ammonia, nitrate, dissolved oxygen, salinity, organic/inorganic phosphorus, MERCURY for simulation of mercury and HEAT for simulation of temperatures in water bodies.

WASP has been applied to various surface water systems, addressing a range of environmental contaminants. Recently, Shabani et al. (2021) simulated flood-induced soil, sediment, and contaminant transport by using a coupled hydrodynamic (HEC-RAS 2D) and water quality model (WASP). Wool et al. (2020) summarized the evolution of the model over the years. Some applications of WASP include : nutrient loading on water quality in Tampa Bay, Florida (Wang et al., 1999); mercury fate and transport in the Carson River, Nevada

(Carroll et al., 2000); impacts of climate change on water quality of Chungju Lake (South Korea) (Park et al., 2013); and the effects of increasing temperature and solar radiation due to climate change on water quality of the Sitalakhya River (Bangladesh) for the years 2009, 2030, 2050 and 2070 (Alam et al., 2013); the effects of air quality policy changes on water quality (Burian et al., 2022); the effects of farmland withdrawal water on the water quality (dissolved oxygen in the Danshui and Chungkang Rivers, Taiwan (Chen et al., 2012); algal dynamics in an urban river in Beijing (Jia et al., 2010); dissolved oxygen depletion in diverted floodwaters of the Elbe River, Germany (Lindenschmidt et al., 2009); eutrophication control in the Keban Dam Reservoir, Turkey (Soyupak et al., 1996); eutrophication control in El Pañe Reservoir (Larico et. al, 2019). Elçi et al. (2010), applied the WASP model to investigate the effects of Kizildere Geothermal Power Plant discharges on the water quality of the B. Menderes River. Kannel and Gan (2013), applied the WASP model to investigate the potential impacts of oil sand processed water in terms of water quality by dividing the Athabasca River water body into 46 rectangular segments. The model was also applied to simulate various copper effluent control measures and impacts of the heavy rainfall by the climate change on copper concentrations by dividing the mainstream of Erren River into 189 segments (Chueh et. al, 2021). Obin et al. (2021) implemented the model to simulate the water quality concentrations such as; chemical oxygen demand (COD), ammonium nitrogen (AN) and total phosphorus (TP) and predict the water environmental capacity in Lushui River, China. Seo et al. (2012), predicted chlorophyll-a changes due to weir constructions by dividing the Nakong river, South Korea into eleven reaching. Iqbal et al. (2018) investigated the effects of the physical geometry of wastewater-treatment facilities on pollution concentrations in Ravi River (Pakistan) by dividing the river into eighteen segments.

In this study, for the application of the WASP model to predict water quality parameters, Porsuk river is divided into 25 segments and location and physical properties of each segment are defined respectively in Table 1.

Table 1. Location and physical properties of the main river segments used in the model

Segment No	X coordinate	Y coordinate	Segment Name	Length (m)	Width (m)	Slope (θ)
2	39.07876	30.1808	Altintas Village- Zafer Airport	8569.3	6.9	0.00082
3	39.11447	30.11463	Zafer Airport-Haydarlar Intake	15405.5	25.7	0.00045
4	39.19748	29.99047	Haydarlar-Adakoyu Route	3091.5	14.8	0.00032
5	39.20738	29.9687	Adakoyu Route-Ada	7647.4	13.7	0.00026
6	39.26397	29.98031	Ada-Agackoy	20000.0	15.2	0.00260
7	39.38014	30.06653	Agackoy- Calca	20000	22.95	0.00105
8	39.46242	30.02649	Calca-Kutahya Intake	15210.4	24.8	0.00092
9	39.55533	30.06802	Kutahya Outlet-Reservoir1	12468.5	77.3	0.00128
10	39.586	30.14198	Reservoir1-Reservoir2	6046	1363.2	0
11	39.62566	30.17688	Reservoir2-Reservoir3	5845.7	1724.1	0
12	39.63312	30.23757	Reservoir3-Eskisehir Intake	20000	54	0.0026
13	39.64833	30.36753	Eskisehir Intake-Esenkara	20000	21.42	0.0012
14	39.72944	30.4248	Esenkara-Eskisehir Outlet	20000	23.78	0.0012
15	39.77156	30.55555	Eskisehir Outlet-Cavkum	20000	24.5	0.0006
16	39.81572	30.71093	Cavkum-Alpu Intake	20000	18.7	0.0005
17	39.77813	30.93529	Alpu Intake-Alpu	2693.8	18.4	0.00037
18	39.76836	30.96016	Alpu-Guroluk	20000	20.1	0.00015
19	39.68892	31.10943	Guroluk-Beylikova	12229.3	15.3	0.00049
20	39.68423	31.20469	Beylikova-Yalinli	20000	22.4	0.00055
21	39.69572	31.37774	Yalinli-Yunusemre	12404.1	18.9	0.00048
22	39.70131	31.47751	Yunusemre-Bicer Intake	20000	17.4	0.0009
23	39.71313	31.62732	Bicer Intake-Outlet	20000	13.1	0.0011
24	39.66823	31.72424	Bicer Outlet-Sazilar	20000	12.7	0.00075
25	39.67838	31.9709	Sazilar-Sakarya	2370.1	13.4	0.00338

The river segmentation is performed based on monitoring stations where water quality data are available in the literature (Köse et al., 2016) and at the stations where flow rates are monitored regularly (Figure 1). Prior to the simulation of water quality parameters, simulation results of the hydrodynamics along the river are validated with the available observations. For these simulations, the eutrophication module (EUTRO) is selected, and 1-D kinematic wave approach is utilized. The maximum time step is set to 2.46 minutes in the simulations. The flow rates are output at all stations daily for the simulation period (10/1/2014-9/30/2015). For the model domain, the segments are specified as input based on the properties summarized in Table 1. The parameters measured at the stations at the beginning of the simulation period are specified in the model as initial conditions. The daily values of air temperature, wind speed, solar radiation, and water temperature are provided as input data for the simulation period.

The model is calibrated using the following parameters (Table 2) based on the literature (Larico and Medina, 2019).

Table 2. Kinetic constants for WASP model calibration (Larico and Medina, 2019).

Parameters	Calibrated Value
Global Constant	
Fresh water = 0 - Marine Water = 1	0
Ks Option	1
Salinity Simulation Option (1 = Salinity- 2 = TDS)	1
Water Temperature	
Heat exchange option (0=full heat balance- 1=equilibrium temperature)	0
Sediment (ground) temperature- °C	10
Ice switch (0 = no ice solution- 1=ice solution- 2=detailed ice solution)	0
Inorganic Nutrient Kinetics	
Nitrification Rate Constant at 20 degree C (1/day)	0.425
Nitrification Temperature Coefficient	1
Half Saturation Constant for Nitrification Oxygen Limit (mg O2/L)	1.00E-06
Minimum Temperature for Nitrification Reaction (degree C)	7
Denitrification Rate Constant at 20 degree C (1/day)	0.01
Denitrification Temperature Coefficient	1
Half Saturation Constant for Denitrification Oxygen Limit (mg O2/L)	1.00E-06
Organic Nutrients	
Dissolved Organic Phosphorus Mineralization Rate Constant at 20 C (1/day)	0
Dissolved Organic Phosphorus Mineralization Temperature Coefficient	1
Dissolved Oxygen	
Global Reaeration Rate Constant at 20 C (1/day)	5
Oxygen to Carbon Stoichiometric Ratio	2.667
Theta -- Reaeration Temperature Correction	1.024
Theta -- SOD Temperature Correction	1.04

After calibration of the kinematic constants, the comparison of simulated water temperatures and observed water temperatures which were obtained from Kose et. al, 2016, are given in Table 3.

Table 3. Comparison of simulated and observed water temperature values

Segment No	Segment Name	Simulated Water Temperature (July) (°C)	Observed Water Temperature (°C)
1	Beskaris-Altintas Village	17.9	18.1
6	Ada-Agackoy	23.0	22.8
7	Agackoy-Calca	22.2	22
9	Kutahya outlet-Reservoir 1	23.8	24
10	Reservoir 1- Reservoir 2	24.1	23.9
11	Reservoir 2- Reservoir 3	23.6	23.5
12	Reservoir 3- Eskisehir Intake	23.7	23.9
13	Eskisehir Intake-Esenkara	14.6	14.5
18	Alpu Outlet-Guroluk	21.1	21.3
20	Beylikova-Yalinli	23.4	23.4
22	Yunusemre-Bicer Intake	25.3	25.4
25	Sazilar-Sakarya	24.9	25

The RMSE and MAE values for the comparison are calculated as 0.13 °C (0.6% of the average temperature), and 0.15 °C (0.6% of the average temperature), respectively.

3. Results

3.1 Simulation of the Hydrodynamics

At inflow section, the flow functions showing flow time series at the boundaries of the model are specified using daily flow measurements recorded at the river monitoring stations. As shown previously in Figure 1, eight different flow functions are defined. Figure 9 presents the comparison of simulated flow rates with the observations for six different stations: Beskaris, Porsuk Ciftligi, Calca, Esenkara, Parsibey and Kiranharmani stations.

Error analysis is conducted to evaluate the errors between the predicted and observed discharge time series. The Root Mean Square Error (RMSE) and Mean Absolute Error (MAE) used to examine the difference between the observed and measured discharge time series are given as in Eq. (2) and Eq. (3):

$$RMSE = \sqrt{\sum_{i=1}^{n} \frac{\left(Q_{observed} - Q_{predicted}\right)^2}{n}} \quad (2)$$

$$MAE = \frac{1}{n}\sum_{i=1}^{n} \left| Q_{observed} - Q_{predicted} \right| \quad (3)$$

where *RMSE* is root mean square error, while *MAE* is mean absolute error. The calculated RMSE and MAE values for each station are given in Table 4.

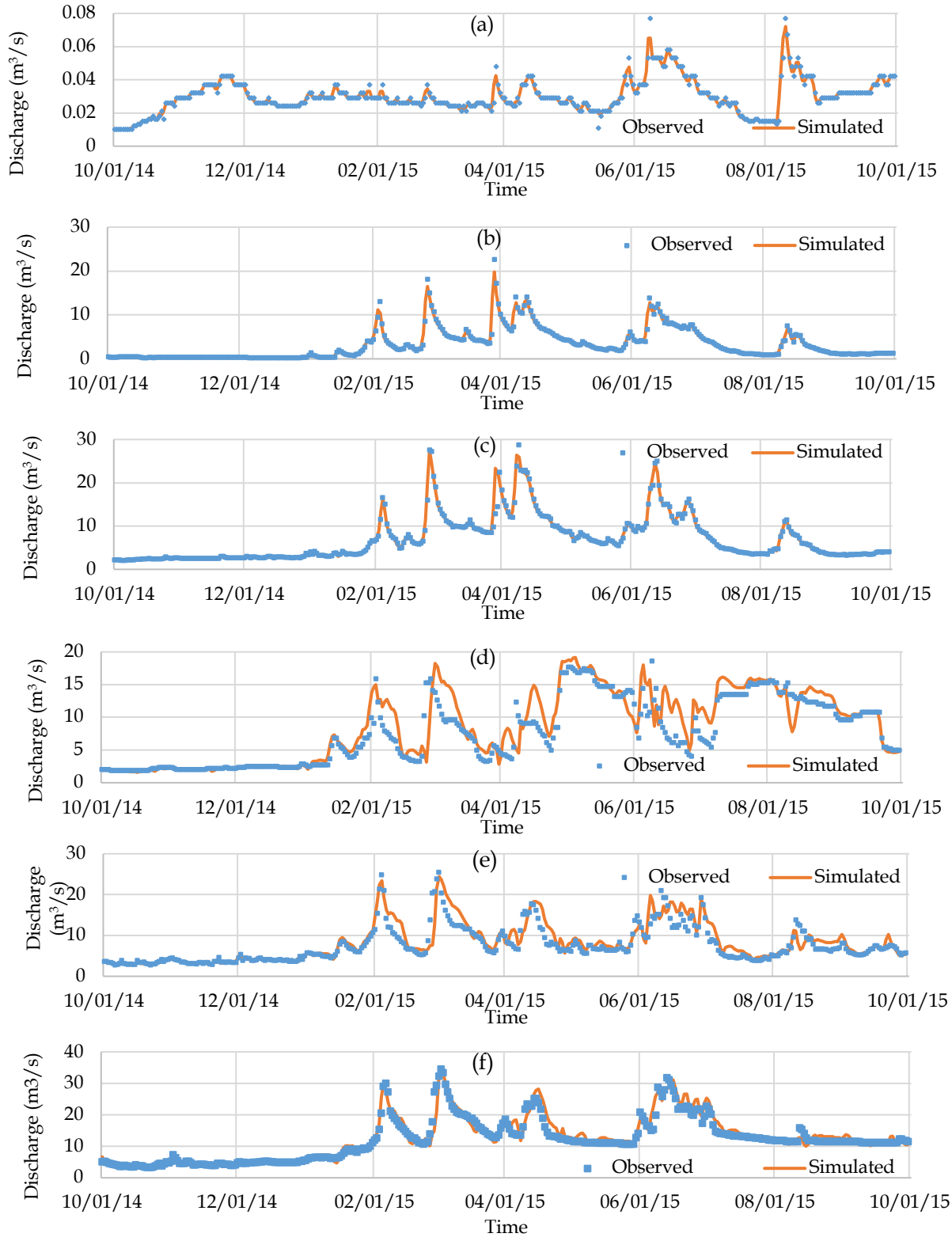

Figure 9. Comparison of flow rates at six stations;; a) Beskaris, b) Porsuk Ciftligi, c) Calca, d) Esenkara, e) Parsibey, f) Kiranharmani stations

Compared to the stations upstream of the river, higher RMSE values are calculated for Esenkara and Parsibey stations: 2.415 m^3/s (13% of the maximum discharge), and 2.088 m^3/s (8.2% of the maximum discharge), respectively (Table 3).

Table 4. RMSE and MAE values for discharge stations

Stations	Root Mean Square Error (RMSE)	Mean Absolute Error (MAE)
Beskaris	0.002	0.001
Porsuk Ciftligi	0.718	0.260
Calca	0.918	0.313
Esenkara	2.415	1.555
Parsibey	2.088	1.324
Kiranharmani	1.823	1.172

Next, we compared the simulated water temperatures with the observed ones (Figure 10). The RMSE and MAE values are calculated as 2.57˚C (11% of the maximum temperature) and 1.89 ˚C (8% of the maximum temperature), indicating that water temperatures are predicted reasonably for the purposes of the study.

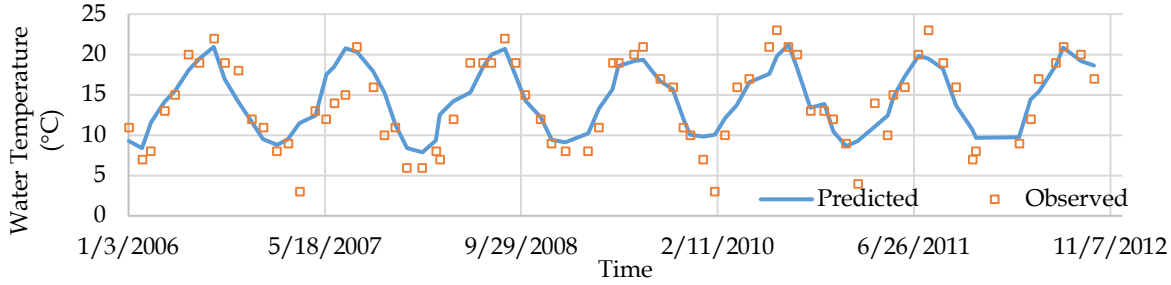

Figure 10. Comparison of observed water temperatures at Besdegirmen station with the simulated values predicted.

3.2 Simulation of the Water Quality Parameters

Following the simulation of discharges at monitoring stations accurately, water quality parameters are modeled. In the loads section, water quality parameters are specified as input data for the model segments according to sampling locations. The model is run for the water year of 2015 by the eutrophication module and the simulated dissolved oxygen concentrations, phosphorus and nitrate concentrations are compared with the observed values reported by Köse et al., (2016) (Table 5, 6 and 7). The simulated results are also presented along the river (Figure 11).

Table 5. Comparison of simulated and observed dissolved oxygen concentrations

Segment No	Segment Name	Simulated DO (mg/L)	Observed DO (mg/L)
1	Beskaris-Altintas Village	7.89	7.86
6	Ada-Agackoy	7.95	7.97
7	Agackoy-Calca	7.47	7.56
9	Kütahya outlet-Reservoir 1	3.33	3.3
10	Reservoir 1- Reservoir 2	14.19	14.14
11	Reservoir 2- Reservoir 3	13.32	13.24
12	Reservoir 3- Eskisehir Intake	13.83	13.8
13	Eskisehir Intake-Esenkara	7.99	7.92
18	Alpu Outlet-Guroluk	4.36	4.33
20	Beylikova-Yalinli	6.59	6.61
22	Yunusemre-Bicer Intake	5.62	5.66
25	Sazilar-Sakarya	7.93	7.97

Table 6. Comparison of simulated and observed phosphorus concentrations

Segment No	Segment Name	Simulated P (mg/L)	Observed P (mg/L)
1	Beskaris-Altintas Village	0.026	0.027
6	Ada-Agackoy	0.044	0.046
7	Agackoy-Calca	0.033	0.032
9	Kütahya outlet-Reservoir 1	0.293	0.307
10	Reservoir 1- Reservoir 2	0.076	0.074
11	Reservoir 2- Reservoir 3	0.059	0.054
12	Reservoir 3- Eskisehir Intake	0.028	0.026
13	Eskisehir Intake-Esenkara	0.314	0.307
18	Alpu Outlet-Guroluk	0.506	0.503
20	Beylikova-Yalinli	0.486	0.478
22	Yunusemre-Bicer Intake	0.504	0.498
25″	Sazilar-Sakarya	0.55	0.53

Table 7. Comparison of simulated and observed nitrate concentrations

Segment No	Segment Name	Simulated Nitrate (mg/L)	Observed Nitrate (mg/L)
1	Beskaris-Altintas Village	0.990	1.05
6	Ada-Agackoy	0.604	0.609
7	Agackoy-Calca	1.000	1.01
9	Kütahya outlet-Reservoir 1	0.903	0.91
10	Reservoir 1- Reservoir 2	0.152	0.158
11	Reservoir 2- Reservoir 3	0.342	0.342
12	Reservoir 3- Eskisehir Intake	0.232	0.228
13	Eskisehir Intake-Esenkara	0.638	0.631
18	Alpu Outlet-Guroluk	2.76	2.76
20	Beylikova-Yalinli	3.23	3.25
22	Yunusemre-Bicer Intake	3.39	3.38
25	Sazilar-Sakarya	2.92	2.98

The RMSE values for the comparison are calculated as 0.11 mg/L (1.3% of the average concentration) for the dissolved oxygen, 0.04 mg/L (16.8% of the average concentration) for phosphorus, 0.058 mg/L (4% of the average concentration) for nitrate.

Following this analysis, simulation results are also compared for two times of the year having very different flow regimes. Monthly averaged July and January concentrations are selected for this purpose. These periods are selected since the rivers is expected to have the lowest (July) and the highest (January) dissolved oxygen concentrations during these times of the year. Table 5 shows the concentrations predicted at different segments along the stream. Comparison of the simulation results indicated that in both months, lowest dissolved oxygen values are observed at specific locations: Kutahya-Reservoir1 segment 3.33 mg/L (Red dot), and at Alpu-Guroluk segment as 4.36 mg/L. At these stations simulated and observed dissolved oxygen values were below 5 mg/L throughout the year.

Next, the total phosphorus and nitrate concentrations along the stream for the two months: January and July were simulated. A significant increase in the observed/simulated total phosphorus is observed from 0 to 0,3 mg/l at the Kutahya-Reservoir1 segment and from 0,3 mg/L to 0,5 mg/l at the Alpu-Guroluk segment. As for the nitrate concentrations, a significant increase is observed from 0,63 mg/L to 2.76 mg/l at the Alpu-Guroluk segment.

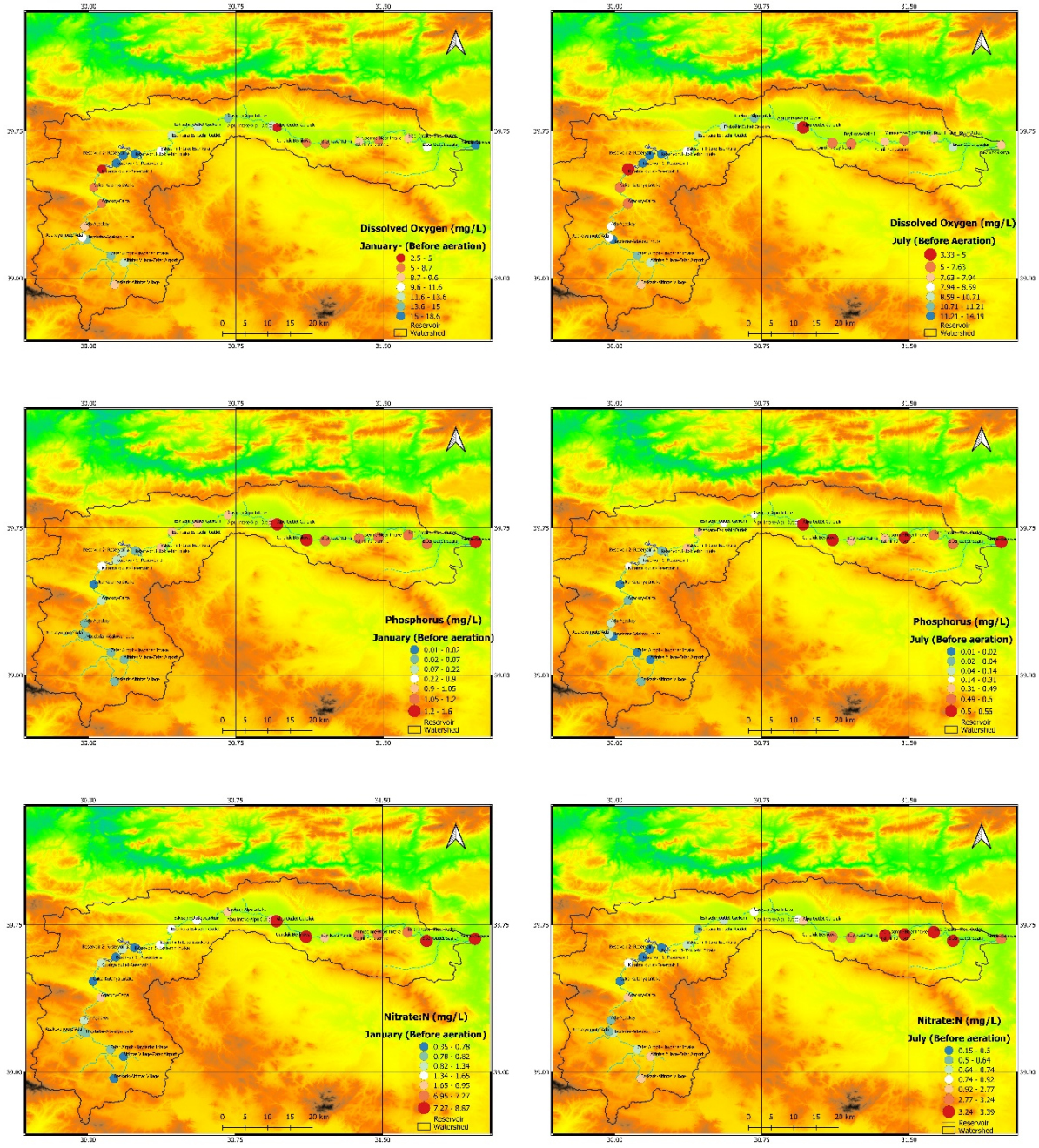

(a) (b)

Figure 11. Comparison of the simulated dissolved oxygen, phosphorus, and nitrate concentrations along the river for two different months; a) January, b) July

3.3 Proposed mitigation solution for the improvement of the water quality: Aeration

Aeration/oxygenation has been widely used to improve water quality associated with eutrophic conditions in water systems. In general, it is regarded as a good solution to prevent blooms of cyanobacteria because it reduces light availability (Beutel and Horne 1999).Various forms of hypolimnetic aeration/oxygenation systems have been installed to the lakes/reservoirs with varying degrees of success in the past (Holland and Tate, 1984; Gallagher, 1984; Meyer et al., 1992; Burns and Powling, 1981; Croome, 1981; Chipofya and Matapa, 2003; Horne, 2019; Horne and Beutel, 2019). A successful application of a hypolimnetic oxygenation system was utilized in a hatchery on the Mokelumne River,

California, following the death of 300,000 salmonid hatchery fish, suspectively by Hydrogen sulfide (H2S). Following the oxygenation operation, Chinook salmon returns rose significantly (Horne, 2019). In another application, long-term improvement in water quality was achieved by a hypolimnetic oxygenation system in Camanche Reservoir, California, a eutrophic reservoir, experiencing blooms of cyanobacteria. Within days of the application, water quality improved and hypolimnion phosphate and ammonium concentrations declined as stated in Horne and Beutel (2019). The previous design of artificial destratification systems was based on trial and error in the site, where neither the effect of air bubble size nor the effect of air density in the bubble plume could be investigated.

Following the successful applications in the literature, installations of aeration systems to two segments observed to have the lowest dissolved oxygen concentrations have been proposed in this study. The first aeration point is selected "Kütahya outlet-Reservoir1" segment (#9) to increase the dissolved oxygen concentrations to the maximum concentration value (14.2 mg/L) and to examine the effects of this change on the following segments. The simulated dissolved oxygen concentrations at the segments along the river, after the first aeration applied at "Kutahya outlet-Reservoir1" segment is given in Table 8. Based on the simulated results it was observed that beginning with the "Alpu Outlet-Guroluk" segment (#18) dissolved oxygen concentrations experience a sharp decrease and fall below 5 mg/L indicating of decreased water quality at the stretch of the river. Therefore, a second aeration is applied at this segment. Table 9 presents the results of the proposed aeration applied at two segments and gives a comparison of the simulated dissolved oxygen, phosphorus and nitrate concentrations for summer (July) and winter (January) before and after the application of the aeration. The simulated results are also presented along the river (Figure 12). As can be seen in Table 9, aeration at two segments has significantly improved the dissolved oxygen concentrations, whereas it has a more subtle effect on nitrate and phosphorus concentrations.

Table 8. The first aeration effects on the following segments

Segment No	Segment Name	Simulated DO-July (mg/L)	Simulated DO-January (mg/L)
1	Beskaris-Altintas Village	7.89	9.42
2	Altintas Village-Zafer Airport	10.71	13.59
3	Zafer Airport -Haydarlar Intake	11.20	14.53
4	Haydarlar-Adakoyu route	11.21	14.56
5	Adakoyu route-Ada	8.09	9.80
6	Ada-Agackoy	7.95	9.54
7	Agackoy-Calca	7.47	7.82
8	Calca-Kutahya Intake	5.94	6.18
9	Kutahya outlet-Reservoir 1	14.20	18.80
10	Reservoir 1- Reservoir 2	23.20	32.20
11	Reservoir 2- Reservoir 3	22.32	32.6
12	Reservoir 3- Eskisehir Intake	19.9	24.5
13	Eskisehir Intake-Esenkara	10.9	16.8
14	Esenkara-Eskisehir Outlet	10.2	14.5
15	Eskisehir Outlet-Cavkum	10.8	14.5
16	Cavkum-Alpu Intake	11.03	14.2
17	Alpu Intake-Alpu Outlet	11.04	14.2
21	Yalinli-Yunusemre	7.79	9.19
22	Yunusemre-Bicer Intake	5.71	7.18
23	Bicer Intake- Bicer Outlet	7.8	9.55
24	Bicer Outlet-Sazilar	8.84	10.95
25	Sazilar-Sakarya	7.96	15.41

Table 9. Comparison of the simulated dissolved oxygen, phosphorus and nitrate concentrations for summer (July) and winter (January) before and after the application of the aeration (segments 1-25)

Segment No	1	2	3	4	5	6	7	8
DO (mg/L)								
(July)- Before the aeration	7.89	10.71	11.20	11.21	8.09	7.95	7.47	5.94
(July)- After the aeration	7.89	10.71	11.20	11.21	8.09	7.95	7.47	5.94
(Jan)- Before the aeration	9.42	13.59	14.53	14.56	9.80	9.54	7.82	6.18
(Jan)- After the aeration	9.42	13.59	14.53	14.56	9.80	9.54	7.82	6.18
P (mg/L)								
(July)- Before the aeration	0.03	0.02	0.02	0.02	0.05	0.04	0.03	0.01
(July)- After the aeration	0.03	0.02	0.02	0.02	0.05	0.04	0.03	0.01
(Jan)- Before the aeration	0.02	0.02	0.02	0.02	0.05	0.05	0.10	0.02
(Jan)- After the aeration	0.02	0.02	0.02	0.02	0.05	0.05	0.10	0.02
N (mg/L)								
(July)- Before the aeration	0.99	0.93	0.72	0.71	0.63	0.60	1.00	0.35
(July)- After the aeration	0.99	0.93	0.72	0.71	0.63	0.60	1.00	0.35
(Jan)- Before the aeration	0.78	0.78	0.81	0.82	0.81	0.85	2.98	0.51
(Jan)- After the aeration	0.78	0.78	0.81	0.82	0.81	0.85	2.98	0.51

Segment No	9	10	11	12	13	14	15	16
DO (mg/L)								
(July)- Before the aeration	3.33	14.19	13.32	13.83	7.99	9.05	10.35	10.94
(July)- After the aeration	14.20	23.20	22.32	19.90	10.90	10.20	10.80	11.03
(Jan)- Before the aeration	2.66	18.53	17.86	17.71	10.44	11.92	13.21	13.75
(Jan)- After the aeration	18.80	32.20	32.60	24.50	16.80	14.50	14.50	14.20
P (mg/L)								
(July)- Before the aeration	0.29	0.08	0.06	0.03	0.31	0.31	0.31	0.31
(July)- After the aeration	0.22	0.06	0.05	0.02	0.30	0.27	0.27	0.27
(Jan)- Before the aeration	0.40	0.14	0.14	0.07	0.91	0.92	0.93	0.94
(Jan)- After the aeration	0.30	0.11	0.11	0.05	0.62	0.78	0.79	0.80
N (mg/L)								
(July)- Before the aeration	0.90	0.15	0.34	0.23	0.64	0.63	0.72	0.80
(July)- After the aeration	0.77	0.19	0.33	0.23	0.58	0.57	0.65	0.72
(Jan)- Before the aeration	1.33	0.37	0.83	0.48	1.37	1.62	1.64	1.66
(Jan)- After the aeration	1.13	0.42	0.79	0.47	1.22	1.47	1.49	1.51

Segment No	17	18	19	20	21	22	23	24	25
DO (mg/L)									
(July)- Before the aeration	10.71	4.36	6.62	6.59	7.66	5.62	7.72	8.79	7.93
(July)- After the aeration	11.04	14.20	14.90	11.60	11.70	9.50	8.96	8.92	8.20
(Jan)- Before the aeration	12.99	3.85	7.40	6.98	8.93	6.98	9.41	10.89	15.36
(Jan)- After the aeration	14.20	21.60	23.70	13.30	14.30	12.70	12.20	12.10	16.80
P (mg/L)									
(July)- Before the aeration	0.31	0.51	0.51	0.49	0.49	0.50	0.50	0.50	0.55
(July)- After the aeration	0.27	0.41	0.41	0.39	0.39	0.42	0.43	0.44	0.51
(Jan)- Before the aeration	0.94	1.57	1.59	1.06	1.07	1.09	1.10	1.10	1.52
(Jan)- After the aeration	0.80	1.27	1.28	0.86	0.86	0.88	0.89	0.90	1.34
N (mg/L)									
(July)- Before the aeration	0.81	2.76	2.86	3.23	3.24	3.39	3.35	3.32	2.92
(July)- After the aeration	0.73	2.19	2.27	2.62	2.63	2.76	2.77	2.78	2.61
(Jan)- Before the aeration	1.74	8.28	8.87	6.94	6.99	7.18	7.24	7.29	8.53
(Jan)- After the aeration	1.51	6.63	7.11	5.65	5.68	5.86	5.90	5.94	7.39

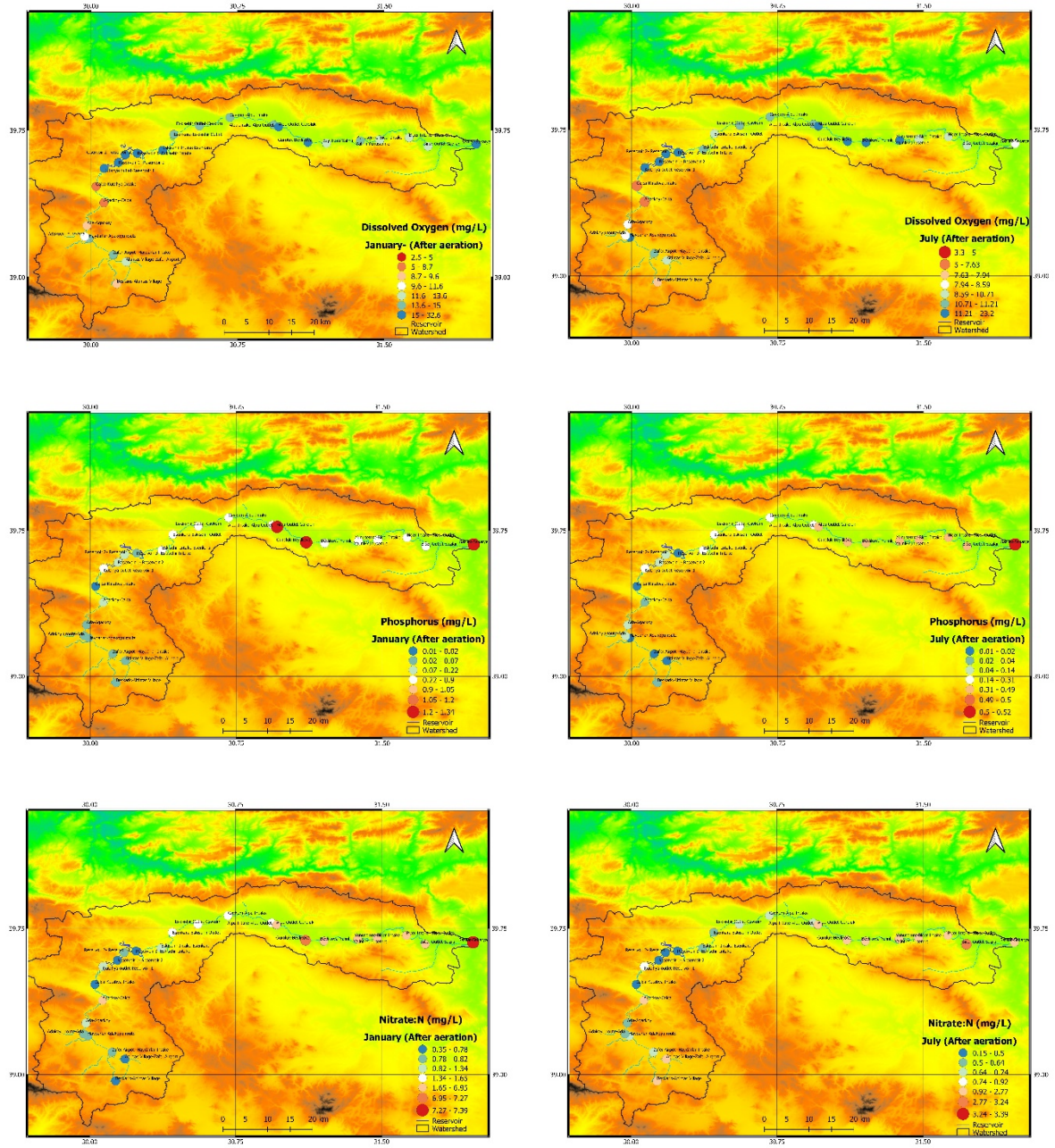

(a) January (b) July

Figure 12. Comparison of the simulated dissolved oxygen, phosphorus, and nitrate concentrations along the river for two different months; a) January, b) July after aeration is applied to the segments.

3.4 Modeling of Chlorophyll-a

Phytoplankton is usually included as a state variable in water quality models such as WASP because of their effects on dissolved oxygen concentrations. When phytoplankton populations exceed established limits, this can be an environmental concern, although the other forms of algae are of equal or greater importance in many water bodies. In this study, the changes in chlorophyll-a concentrations were simulated via the eutrophication module before and after the aeration is applied as mitigation solution in the study site. The calibrated kinematic constants used in modeling of the chlorophyll-a concentrations are given in Table 10.

Table 10. Kinetic constants for modeling of chlorophyll for WASP model calibration (Larico and Medina, 2019)

Parameters	Calibrated Value
Phytoplankton Maximum Growth Rate Constant at 20 C (1/day)	3.5
Phytoplankton Growth Temperature Coefficient	1.068
Phytoplankton Carbon to Chlorophyll Ratio (mg C/mg Chl)	50
Optimal Temperature for Growth (C)	20
Shape parameter for below optimal temperatures	0.004
Shape parameter for above optimal temperatures	0.01
Phytoplankton Respiration Rate Constant at 20 C (1/day)	0.08
Phytoplankton Respiration Temperature Coefficient	1.045
Phytoplankton Death Rate Constant (Non-Zoo Predation) (1/day)	0.1
Nitrogen fixation option (0 no- 1=yes)	1
Phytoplankton Optimal Light Saturation as PAR (watts/m2)	300
Phytoplankton Half-Sat. for Mineralization Rate (mg Phyt C/L)	0.001
Phytoplankton Half-Saturation Constant for N Uptake (mg N/L)	0.4
Phytoplankton Half-Saturation Constant for P Uptake (mg P/L)	0.08
Phytoplankton Half-Saturation Constant for Si Uptake (mg Si/L)	0.1
Phytoplankton Detritus to Carbon Ratio (mg D/mg C)	2.5
Phytoplankton Nitrogen to Carbon Ratio (mg N/mg C)	0.25

Comparison of the simulated chlorophyll-a concentrations before and after the aerations for July and January (Table 11, Figures 13 and 14) indicates a slight decrease in the simulated concentrations after the aeration. The average of simulated chlorophyll-a concentrations for the stream decreased from 1 mg/l to 0.95 mg/l for July and decreased from 1.59 mg/l to 1.42 mg/l for January. Since the aeration was applied after the" Kutahya outlet-Reservoir1" segment (#9), higher values of chlorophyll-a concentrations observed at the upstream stations (1,2,5,6) were not affected.

Table 11. Comparison of the simulated chlorophyll-a concentrations before and after the aerations for July and January

Segment No	Segment Name	Chlorophyll-a-July (mg/L) Before the aeration	Chlorophyll-a-July (mg/L) After the aeration	Chlorophyll-a-January (mg/L) Before the aeration	Chlorophyll-a-January (mg/L) After the aeration
1	Beskaris-Altintas Village	3.05	3.05	2.66	2.66
2	Altintas Village-Zafer Airport	2.17	2.17	2.16	2.16
3	Zafer Airport -Haydarlar Intake	0.92	0.92	1.15	1.15
4	Haydarlar-Adakoyu route	0.76	0.76	1.06	1.06
5	Adakoyu route-Ada	3.35	3.35	3.38	3.38
6	Ada-Agackoy	2.86	2.86	3.67	3.67
7	Agackoy-Calca	0.92	0.92	2.88	2.88
8	Calca-Kutahya Intake	0.54	0.54	0.79	0.79
9	Kutahya outlet-Reservoir 1	0.71	0.53	1.02	0.47
10	Reservoir 1- Reservoir 2	0.27	0.12	0.68	0.22
11	Reservoir 2- Reservoir 3	0.23	0.12	0.49	0.12
12	Reservoir 3- Eskisehir Intake	0.42	0.34	0.56	0.4
13	Eskisehir Intake-Esenkara	0.48	0.39	0.86	0.74
14	Esenkara-Eskisehir Outlet	0.33	0.27	0.86	0.78
15	Eskisehir Outlet-Cavkum	0.32	0.28	0.82	0.76
16	Cavkum-Alpu Intake	0.3	0.28	0.78	0.76
17	Alpu Intake-Alpu Outlet	0.38	0.37	1.06	1.05
18	Alpu Outlet-Guroluk	0.83	0.67	2.36	1.64
19	Guroluk-Beylikova	0.8	0.66	2.28	1.82
20	Beylikova-Yalinli	0.82	0.72	1.6	1.28
21	Yalinli-Yunusemre	0.95	0.88	1.72	1.38
22	Yunusemre-Bicer Intake	1.07	1.01	1.82	1.47
23	Bicer Intake- Bicer Outlet	1.02	0.98	1.76	1.57
24	Bicer Outlet-Sazilar	0.96	0.92	1.69	1.66
25	Sazilar-Sakarya	0.53	0.52	1.57	1.53

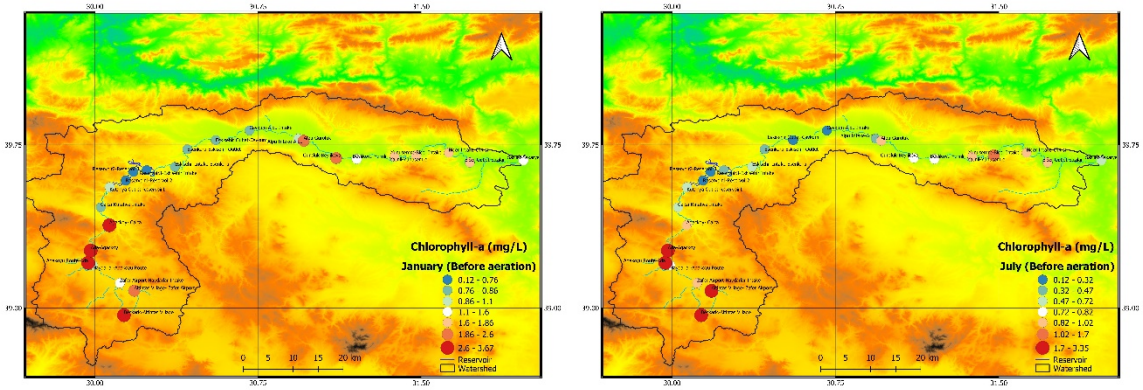

(a) January (b) July

Figure 13. Comparison of the simulated chlorophyll-a concentrations along the river for two different months; a) January, b) July before aeration.

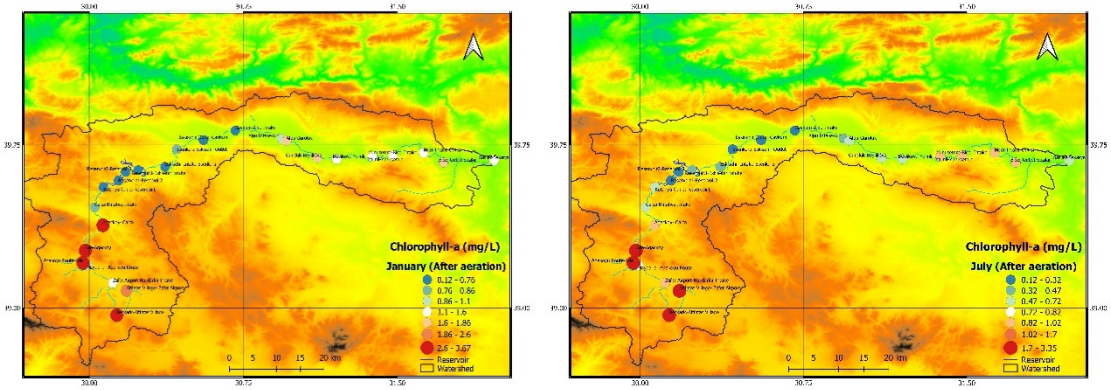

(a) January (b) July

Figure 14. Comparison of the simulated chlorophyll-a concentrations along the river for two different months; a) January, b) July after aeration is applied to the segments.

4. Conclusions

In this study, hydrodynamics and water quality parameters are simulated in the Porsuk River via the application of WASP for the water year 2015. The Porsuk main river is divided into 25 segments, considering available water quality and flow monitoring stations. For calibration of the model, the flow rates monitored at Beskaris, Porsuk Ciftligi, Calca, Esenkara, Parsibey and Kiranharmani stations are used. Following the simulation of discharges at the flow gauging stations accurately, water quality parameters are modeled via the eutrophication module available within the WASP model.

Based on the observed data and the numerical simulations, it can be concluded that the water quality in the Porsuk river is better in the upstream reaches but starts to deteriorate after passing through the province of Kütahya. Dissolved oxygen observations and the numerical model simulations indicate a sudden decrease from 7.56 mg/l to 2.6 mg/l along segment #9.

Water quality then gets better at the reservoir but then another sudden decrease is observed at further downstream at the Alpu-Guroluk segment. Comparison of the simulation results for dissolved oxygen indicated that in both January and July having very different flow regimes, the lowest dissolved oxygen values are observed at specific locations: Kutahya-Reservoir1 segment concentrations of dissolved oxygen are observed as 2.66 in January and 3.33 mg/L in July respectively, and at Alpu-Guroluk (#18) segment as 4.36 mg/L in both months. At these stations, dissolved oxygen stays below the standard limit of 5 mg/L throughout the year.

As a mitigation option, aeration applications at these two stations are proposed and the effects of aeration on the simulated parameters of dissolved oxygen, phosphorus and nitrate concentrations are investigated. Aeration at two segments has significantly improved the dissolved oxygen concentrations whereas it has a more subtle effect on nitrate and phosphorus concentrations.

We also modeled chlorophyll-a concentrations along the stream based on the calibrated flow and water quality model. However, since no observations of chlorophyll-a concentrations is available, simulated data could not be validated. Still, the simulated chlorophyll-a concentrations before and after aeration can be used for evaluating the effects of the aeration. Comparison of the simulated chlorophyll-a concentrations before and after the aeration for July and January indicated a slight decrease in the simulated concentrations after the aeration. The average of simulated chlorophyll-a concentrations for the stream decreased from 1 mg/l to 0.95 mg/l for July and decreased from 1.59 mg/l to 1.42 mg/l for January. These results can be evaluated as an improvement in water quality.

Author Statement

The authors confirm contribution to the paper as follows: study conception and design: Emre Dumlu; data collection: Emre Dumlu; analysis and interpretation of results: Emre Dumlu, Şebnem Elçi; draft manuscript preparation: Emre Dumlu, Şebnem Elçi. All authors reviewed the results and approved the final version of the manuscript.

Conflict of Interest

The authors declare no conflict of interest.

References

Ambrose, R.B., Wool, T., & Martin, J.L. (1993). WASP User's Manual, US Environmental Protection Agency, *Environmental Research Laboratory*, Athens, Georgia.

Alam, A., Badruzzaman, A. B. M., & Ali, M. A. (2013). Assessing Effect of Climate Change on The Water Quality of The Sitalakhya River Using WASP Model. *J. Civ. Eng*, 41, 21-30.

Beutel, M.W., & Horne, A.J. (1999). A Review of The Effects of Hypolimnetic Oxygenation on Lake and Reservoir Water Quality. *Lake and Reservoir Management*, 15(4), 285-297.

Burian, S.J., McPherson, T.N., Brown, M.J., Streit, G.E., & Turin, H.J. (2002). Modeling the Effects of Air Quality Policy Changes on Water Quality in Urban Areas. *Environmental Modeling & Assessment*, 7, 179–190. https://doi.org/10.1023/A:1016328822334

Burigato Costa, C.M.d., da Silva Marques, L., Almeida, A.K., Leite, I.Z., & de Almeida, I.K. (2019). Applicability of Water Quality Models Around The World—A Review. *Environ Sci Pollut Res*., 26, 36141–36162 https://doi.org/10.1007/s11356-019-06637-2.

Burns, F.L., & Powling, I.J. (1981). Destratification of Lakes and Reservoirs to Improve. Water Quality. *Proceedings of a Joint United States/Australia seminar and workshop*., Melbourne, Australia, February 19–24.

Carroll, R.W.H., Warwick, J.J., Heim, K.J., Bonzongo, J.C., Miller, J.R., & Lyons, W.B. (2000). Simulation of Mercury Transport and Fate in the Carson River, *Nevada. Ecol. Model*, 125, 255–278.

Chen, C., Lung, W., Li, S., & Lin, C. (2012). Technical Challenges with BOD/DO Modeling of Rivers in Taiwan. *J. Hydro-Environ Res*., 6.

Chipofya, V.H., &Matapa, E.J. (2003). Destratification of an Impounding Reservoir Using Compressed Air-case of Mudi Reservoir, Blantyre, Malawi. *Physics and Chemistry of The Earth*, 28(20-27), 1161-1164.

Chueh, Y.Y., Fan, C., & Huang, Y.Z. (2021). Copper Concentration Simulation in a River by SWAT-WASP Integration and Its Application to Assessing The Impacts of Climate Change and Various Remediation Strategies. *Journal of Environmental Management*, 279, 111613. https://doi.org/10.1016/j.jenvman.2020.111613.

Croome, R.L. (1981). Artificial Destratification of Two South Australian Reservoirs. *Proceedings of the International Symposium on Artificial Destratification*, Melbourne, 1979, AGPS.

Downing, J.A., Watson, S.B., & McCauley, E. (2001). Predicting Cyanobacteria Dominance in Lakes. *Canadian Journal of Fisheries and Aquatic Sciences*, 58, 1905–1908.

Dumlu, E., & Elçi, Ş. (2022). Application of the Wasp Model for Assessment of Water Quality of the Porsuk River, Turkey. In Ş. Elçi & G. Bombar (Eds.). *14th International Conference on Hydroscience and Engineering,* 177–185. https://www.iche2022.org/_files/ugd/21d103_be56d464954b4310a2461ccf02fd83b9.pdf.

Elçi Ş., Erdem A., & Gokcen G. (2010). Numerical Modeling of the Effects of Kizildere Geothermal Power Plant on Water Quality of the Great Menderes River, Turkey. *Balwois*. https://balwois.com/wp-content/uploads/old_proc/ffp-1977.pdf

Gallagher, J.W., & Jr. (1984). Richard B. Russell Dam and Lake Oxygen Injection System, *Proceedings of a Seminar on Applications in Water Quality Control*, US Army Corps of Engineers, Committee on Water Quality, Washington, DC, 184-190.

Havens, K.E. (2008). Cyanobacteria Blooms: Effects on Aquatic Ecosystems. In: *Hudnell HK ed. Cyanobacterial Harmful Algal Blooms: State of The Science and Research Needs,* New York, Springer, 733–747.

Hickey, C.W., & Gibbs, M.M. (2009). Lake Sediment Phosphorus Release Management—Decision Support and Risk Assessment Framework. *New Zealand Journal of Marine and Freshwater Research*, 43(3). 819-856. doi: 10.1080/00288330909510043.

Holland, J. P., & Tate Jr, C. H. (1984). Investigation and Discussion of Techniques for Hypolimnion Aeration/Oxygenation. *Army Engıneer Waterways Experiment Station Vicksburg*, Ms Hydraulics Lab.

Horne A.J. (2019). Hypolimnetic Oxygenation 1: Win–Win Solution for Massive Salmonid Mortalities in a Reservoir Tailwater Hatchery on the Mokelumne River, California. *Lake Reservoir Manage*, 35(3),308–322.

Horne A.J, & Beutel M. (2019). Hypolimnetic Oxygenation 3: An Engineered Switch from Eutrophic to a Meso/Oligo-trophic State in a California Reservoir. *Lake Reservoir Manage*, 35(3),338–353.

Hyenstrand, P., Blomqvist, P., & Petersson, A. (1998). Factors Determining Cyanobacterial Success in Aquatic Systems—A Literature Review. *Archiv für Hydrobiologie (Special Issues)*, 51, 41–62.

Iqbal, M.M., Shoaib, M., & Agwanda, P., & Lee, J.L. (2018). Modeling Approach for Water-Quality Management to Control Pollution Concentration: A Case Study of Ravi River, Punjab, Pakistan. *Water 10*, 8, 1068. https://doi.org/10.3390/w10081068.

Jia, H., Zhang, Y., & Guo, Y. (2010). The Development of a Multi-Species Algal Ecodynamic Model for Urban Surface Water Systems and its Application. *Ecol. Model*, 221, 1831–1838.

Köse, E., Çiçek, A., Emiroğlu, Ö., Tokatlı, C., Uğurluoğlu, A., Başkurt, S., Aksu, S., & Uylaş, M. (2016). Water Quality Assessment of Porsuk Stream Basin. *Biological Diversity and Conservation*, 9, 119-126.

Kannel, P.R., & Gan, T.Y. (2013). Application of WASP for Modelling and Management of Naphthenic Acids along Athabasca River, Alberta, Canada, *Water Air Soil Pollut*, 224, 1764. https://doi.org/10.1007/s11270-013-1764-1.

Lindenschmidt, K.E., Pech, I., & Baborowski, M. (2009). Environmental Risk of Dissolved Oxygen Depletion of Diverted Flood Waters in River Polder Systems-A Quasi-2D Flood Modelling Approach. *Sci. Environ*. 407, 1598–1612.

Meyer, E.B., Price, R.E., & Wilhelms, S.C. (1992). Destratification System Design for East Sidney Lake, New York. Final report for USACE, Miscallenous Paper, W-92-2. 1979. *Australian Government Publishing Service*,Canberra, 915.

Park, J.Y., Park, G.A., & Kim, S.J. (2013). Assessment of Future Climate Change Impact on Water Quality of Chungju Lake, South Korea, Using WASP coupled with SWAT. J. Am. *Water Resour. Assoc.*,49, 1225–1238.

Obin, N., Tao, H., Ge, F., & Liu, X. (2021). Research on Water Quality Simulation and Water Environmental Capacity in Lushui River Based on WASP Model. *Water*, 13, 2819. https://doi.org/10.3390/w13202819.

Seo, D.I., Kim, M.A., & Ahn, J.H. (2012). Prediction of Chlorophyll-a Changes Due to Weir Constructions in The Nakdong River Using EFDCWASP Modelling. *Environ. Eng.* Res, 17, 95−102.

Shabani, A., Woznicki, S. A., Mehaffey, M., Butcher, J., Wool, T. A., & Whung, P.Y. (2021). A Coupled Hydrodynamic (HEC-RAS 2D) and Water Quality Model (WASP) for Simulating Flood-induced Soil, Sediment, and Contaminant Transport, *Journal of Flood Risk Management*, 14(4), e12747. https://doi.org/10.1111/jfr3.12747.

Soyupak, S., Mukhallalati, L., Yemisen, D., Bayar, A., & Yurteri, C. (1996). Evaluation of Eutrophication Control Strategies for the Keban Dam Reservoir. *Ecol. Model*, 97, 99–110.

Tekkanat, I.S., & Sarış, F. (2015). Long-Term Trends Observed in Stream Flows in the Porsuk Stream Basin (in Turkish). *Turkish Journal of Geography*, 64, 69-83.

Wang, Q., Dai, W., Zhao, X., Li, S., & Zhao, Y. (2009). Numerical Model of Thermal Discharge from Laibin Power Plant Based on Mike 21FM. *China Environmental Science*, 22, 332–336.

Wang, P.F., Martin, J., & Morrison, G. (1999). Water quality and eutrophication in Tampa Bay, Florida. Estuar, *Coast. Shelf Sci*. 49, 1–20.

Wool, T., Ambrose, R.B., Jr., Martin, J.L., & Comer, A. (2020). WASP 8: The Next Generation in the 50-year Evolution of USEPA's Water Quality Model. *Water*, 12, 1398. https://doi.org/10.3390/w12051398.